https://doi.org/10.5194/egusphere-2023-1288
Preprint. Discussion started: 22 June 2023

Effects of Sea Level Rise and Tidal Flat Growth on Tidal Dynamics and Geometry of the Elbe Estuary

Tara Mahavadi[1], Rita Seiffert[1], Jessica Kelln[1], Peter Fröhle[2]

[1]Federal Waterways Engineering and Research Institute, Hamburg, 22559, Germany
[2]Hamburg University of Technology, Hamburg, 21073, Germany

Correspondence to: Tara Mahavadi (tara.mahavadi@baw.de)

Abstract. Future global mean sea level rise (*SLR*), will affect coastlines and estuaries in the North Sea and therefore coastal protection as well as local unique ecosystems and important waterways. *SLR* will not only raise water levels, but will also influence tidal- and morphodynamics, which is why the tidal flats of the Wadden Sea can potentially grow to a certain extent with *SLR*. Investigations on the effects of climate change induced *SLR* and corresponding potential bathymetric changes inside of estuaries form an important basis for the identification of vulnerabilities and the development of appropriate adaptation strategies. With the help of a highly resolved hydrodynamic-numerical model of the German Bight, we analyse the influence of potential *SLR* and tidal flat elevation scenarios on tidal dynamics in the Elbe estuary. The results show an increase of tidal range in the Elbe estuary due to *SLR* and further reveal, that tidal flat growth can have no effect, decrease or increase the tidal range relative to sole *SLR*, depending on the location and amount of tidal flat elevation. Further analyses demonstrate, how geometric parameters of the Elbe estuary are changing due to *SLR* and tidal flat elevation. We discuss how these changes in estuarine geometry can be an explanation for the changes in tidal range.

1 Introduction

Future global mean sea level rise (*SLR*), as it is projected for this century (Fox-Kemper et al., 2021), will have a huge impact on coastal areas around the world. It will not only raise water levels, but will also affect, for example, tidal dynamics in several ways. In particular, low-lying coastal areas such as the German Bight and adjacent estuaries are vulnerable to changes due to *SLR*. The German Bight, located in the North Sea, includes a large part of the World's Natural Heritage Site Wadden Sea. The Wadden sea is a geological and ecological unique region, structured into several tidal basins with barrier islands, tidal channels and intertidal area.

Due to tidal flat morphodynamics (Friedrichs, 2011) *SLR* will not only influence tidal dynamics, but also the bathymetry in the German Bight. Changes in tidal dynamics influence net-sediment transport and therefore bathymetry, which in turn influences tidal dynamics. Due to the mutual interdependency between hydrodynamic forces and the coastal profile, a morphodynamic equilibrium is striven towards in theory (Friedrichs, 2011). Investigations show, that most intertidal flats in the German Bight were vertically growing in a rate higher than observed mean sea level rise in the recent past (1998-2016)

https://doi.org/10.5194/egusphere-2023-1288
Preprint. Discussion started: 22 June 2023

(Benninghoff and Winter, 2019). However, facing the future acceleration of *SLR*, is difficult to quantify the amount to which tidal flat growth can keep pace with sea level rise, and it remains questionable, whether present hydromorphodynamic equilibrium will be maintained in the future. Several studies found that tidal flats can potentially grow with *SLR*, if sediment availability is sufficient, but cannot keep pace with high future *SLR* scenarios (Becherer et al., 2018, van der Wegen, 2013, Dissanayake, 2012). A precise prediction of the future morphologic development of the Wadden Sea is difficult, as it does not only depend on the rate of *SLR*, but on several other factors as e.g. vertical sediment structure, sediment availability and potentially changing meteorology. Furthermore, long-term numerical simulations of morphodynamic processes are challenging, because complex small-scale processes need to be parameterised and the spatial resolution of morphodynamic simulations is limited by computing power.

In any case, potential tidal flat growth should be considered when studying *SLR*-scenarios, as it strongly affects tidal dynamics in the Wadden Sea (Wachler et al., 2020; Jordan et al., 2021). *SLR* in the German Bight will cause an increase in tidal prism relative to channel cross-sectional-flow area in tidal basins and therefore an increase of current velocity in the channels, which is counteracted by tidal flat elevation (Wachler et al., 2020). *SLR* can cause a shift of the amphidromic point in the German Bight in eastward direction, which is as well counteracted by tidal flat elevation (Jordan et al., 2021). Due to the changes in amphidromes and current velocity, tidal flat elevation with *SLR* causes an increase in M2-amplitude in the German Bight relative to sole *SLR* (Jordan et al., 2021).

One of the main estuaries in the German Bight is the Elbe estuary, which contains the port of Hamburg and is therefore an important shipping route. The Elbe estuary is the part of the Elbe river extending from the weir in Geesthacht to the North Sea (Figure 5). The weir in Geesthacht is the artificial tidal barrier of the estuary. Further downstream, approximately where the estuary reunites again, after splitting into two branches, lies the port of Hamburg. An artificially deepened fairway is maintained from the port of Hamburg to the North Sea, to allow large container ships to reach Hamburg. The part of the estuary upstream of Hamburg to the town Brunsbüttel includes intertidal areas, the extent of which further increases upstream of Brunsbüttel in the dilating mouth of the estuary (Figure 5). The Elbe estuary is a strongly anthropogenically influenced system (e.g. due to the containment by dikes and the deepening of the fairway). While the tidal range in Cuxhaven, in the mouth of the estuary remained relatively constant at around 3 m, the tidal range in St. Pauli, close to the port of Hamburg increased over the last 100 years (Boehlich and Strotmann, 2019). Nowadays the Elbe estuary is an amplified estuary, where the tidal amplitude increases in upstream direction and reaches its maximum close to the port of Hamburg. Further upstream, where water depth decreases and river discharge becomes more relevant, the tide is damped and tidal amplitude decreases.

The future of the Elbe estuary depends not only on anthropogenic measures implemented on site, but also in particular on sea level rise and its implications. Sea level rise and (resulting) topographic changes will alter estuarine geometry and thus influence the tidal wave propagating into the estuary, which is generally modified by amplification, damping, reflection and distortion. Estuarine geometry hereby denotes the form of the intersection of estuarine bathymetry with characteristic local

https://doi.org/10.5194/egusphere-2023-1288
Preprint. Discussion started: 22 June 2023

parameters of the tide. Understanding the future evolution of tidal dynamics due to sea level rise in heavily utilised estuaries such as the Elbe estuary is important for the development of adaptation measures, e.g. in navigation, port infrastructure and water management.

Several model-based methods are available to address this question. Analytical studies on the behaviour of tides in estuaries have been conducted since many decades (Winterwerp and Wang, 2013). Several studies (e.g. Jay, 1991; Friedrichs and Aubrey, 1994; Savenije et al., 2008; Friedrichs, 2010; van Rijn, 2011) developed, discussed and applied analytical solutions to estimate tidal wave propagation in estuaries by simplifying estuarine geometry and the basic equations and developing scaling parameters to describe the systems, while still including the important effects of intertidal area and channel convergence. In these analytical studies, simplified geometric properties of the studied estuaries are considered by the use of several characteristic parameters.

However, accurate computation of time-depended water levels and current velocities requires the application of advanced numerical models, which can consider various driving forces and their interactions with accurate concepts of energy exchange and a precise implementation of estuarine shape (Khojasteh et al., 2021). The importance of accurate representation of bathymetry in numerical models of shallow coastal systems, is pointed out by Holleman and Stacey (2014) and (Rasquin et al., 2020). Rasquin et al. (2020) find, that the increase of tidal amplitude in the German Bight due to *SLR* can be overestimated, if bathymetric resolution in the model is insufficient. A study by Seiffert and Hesser (2014) investigating the effect of *SLR* on tidal dynamics in the Elbe estuary shows, that *SLR* causes an increase of tidal range in the Elbe estuary. However, this study does not consider the potential vertical growth of tidal flats with *SLR*. Even if the future morphologic development of tidal flats in the German Bight and the Elbe estuary is difficult to predict, potential topographic changes might have a considerable impact on tidal dynamics and should not be neglected.

A downside of advanced numerical models, besides computational time and resources, is the loss of simplicity and hence transparency. Therefore, extensive analysis of the simulation results is necessary to gain a system understanding and to provide an insight on how certain parameters affect others. For this purpose, it can be useful to analyse simplified geometric parameters, which were originally developed in the context of analytical estuary models.

Our objective is to investigate how tidal range along the Elbe estuary is influenced by potential future *SLR* and tidal flat growth scenarios. Tidal range is the double of tidal amplitude and the difference between tidal high water and tidal low water. It is an integral part of the energy flux of a propagating tidal wave. Tidal range in estuaries is closely linked with tidal current velocity, mixing, circulation, sediment transport, water quality and ecosystem communities (Khojasteh et al., 2021). Additionally, it is a parameter which has an influence on navigation in and drainage into the estuary, as well as on the dimensioning of waterfront structures and other hydraulic structures in the estuary HTG (2020).

We investigate not only the effect of sole *SLR* scenarios, but also a bandwidth of corresponding simplified hypothetical tidal flat growth scenarios. In our study scenarios of potential future sea level rise and tidal flat growth scenarios are simulated using

https://doi.org/10.5194/egusphere-2023-1288
Preprint. Discussion started: 22 June 2023

the three-dimensional hydrodynamic-numerical method UnTRIM² (Casulli, 2009) in a regional model of the German Bight, to access the influence on tidal range in the Elbe estuary. The aim of this study is to gain a better understanding of the possible effects of potential *SLR* and tidal flat growth scenarios in the Elbe estuary. In addition to characteristic parameters of the vertical tide, we analyse three parameters of estuarine geometry (mean hydraulic depth, convergence of cross-sectional flow area and relative intertidal area). These geometric parameters, which describe the shape of the estuary in a simplified way, are (equally or in similar form) known from previously mentioned analytical models and are herein used to find explanatory approaches for the changes of tidal dynamics simulated by the advanced hydrodynamic-numerical model.

In the subsequent chapter 2 the applied methods will be described. It includes a short description of the model and the simulated scenarios. Moreover, the analysed geometric parameters of the estuary and their potential influence on tidal range are shortly discussed. In chapter 3 the results of the analysed tidal and geometric parameters for some examined scenarios are displayed and outlined. Chapter 4 includes a discussion on the possible reasons for the detected changes in estuarine geometry, as well as the potential role of changing geometry in the alteration of tidal range in the estuary. Finally, chapter 5 summarises the main findings of this study and their relevance and gives an outlook on open questions for future investigations.

2 Theory and Methods

2.1 Model setup

For this study the three-dimensional hydrodynamic numerical model UnTRIM² (Casulli, 2009) is used, which solves the three-dimensional-shallow water equations and the three-dimensional transport equation for e.g. salt, suspended sediment and heat on an orthogonal unstructured grid (Casulli and Walters, 2000). A special feature of UnTRIM² compared to its predecessor UnTRIM is the subgrid technology, which allows a high resolution of the topography independent of the computational grid (Casulli, 2009). The computational grid cells can be wet, partially wet, or dry, allowing a precise mass balance and a realistic wetting and drying (Sehili et al., 2014), which is important for a realistic representation of the large intertidal areas in the German Bight. The variation of the surface drag coefficient with wind speed is parametrised according to S. D. Smith and E. G. Banke (1975). The generation of wind waves as well as sediment and heat transport are not calculated in the model setup used for this study in order to reduce computational effort.

The regional model we use is very similar to the model used by Rasquin et al. (2020). The model domain covers the German Bight from Terschelling in the Netherlands to Hvide Sande in Denmark including the estuaries Elbe, Weser and Ems with their main tributaries (Figure 1). The model boundary is the dike line which therefore cannot be overflowed. The resolution of the computational grid varies between 5 km at the open boundary to about 100 m in the coastal area and the estuaries. A higher subgrid resolution is used in the Wadden sea region and the estuaries of about 10 to 50 m in the finest part. Throughout the model domain, the vertical grid resolution is 1 m to a depth of 27.5 m and 10 m below that. The topography data of the year 2010 implemented into the model was generated in the EasyGSH-DB project (Sievers et al., 2020).

https://doi.org/10.5194/egusphere-2023-1288
Preprint. Discussion started: 22 June 2023

The atmospheric forcing over the model domain (wind field at 10 m height and surface pressure) is derived from COSMO-REA6 (Bollmeyer et al., 2015). The data is generated and made available by the Hans Ertel Center of the University of Bonn in cooperation with the German Weather Service (DWD) (Bollmeyer et al., 2015). Salinity is set to a constant value of 33 PSU at the open boundary and 0.4 PSU at the upstream boundary of the Elbe estuary.

A spring-neap-cycle in July 2013 with a constant river discharge at the upstream boundary of the Elbe estuary of 600 m³/s is simulated with the German Bight model. The weir in Geesthacht is laid in the model during the simulated period. The selected period and discharge are chosen to estimate changes of average conditions without extreme events. Sea level rise is added at the open boundary of the German Bight Model.

Water level at the seaward open boundary of the German Bight model is provided by the Dutch continental shelf model (*DCSMv6FM*) (Zijl, 2014), a 2-D hydrodynamical model which covers the north-west European shelf and is a further development of *DCSMv6* (Zijl et al., 2013; Zijl et al., 2015) (Figure 1). *DCSMv6FM* is using the flexible mesh technique *D-Flow FM* (DFlow Flexible Mesh) (Kernkamp et al., 2011), which is based on the classical unstructured grid concept. At the seaward open boundary the *DCSMv6FM* is forced by the amplitudes and phases of the 22 main diurnal and semidiurnal constituents which are derived by interpolation from the dataset generated by the GOT00.2 global ocean tide model (Ray, 1999). Sixteen additional partial tides are adopted from FES2012 (Carrère et al., 2013). As for the smaller regional model, the atmospheric forcing for *DCSMv6FM* is derived from *COSMO-REA6* (Hans-Ertel-Centre for Weather Research; (Bollmeyer et al., 2015).

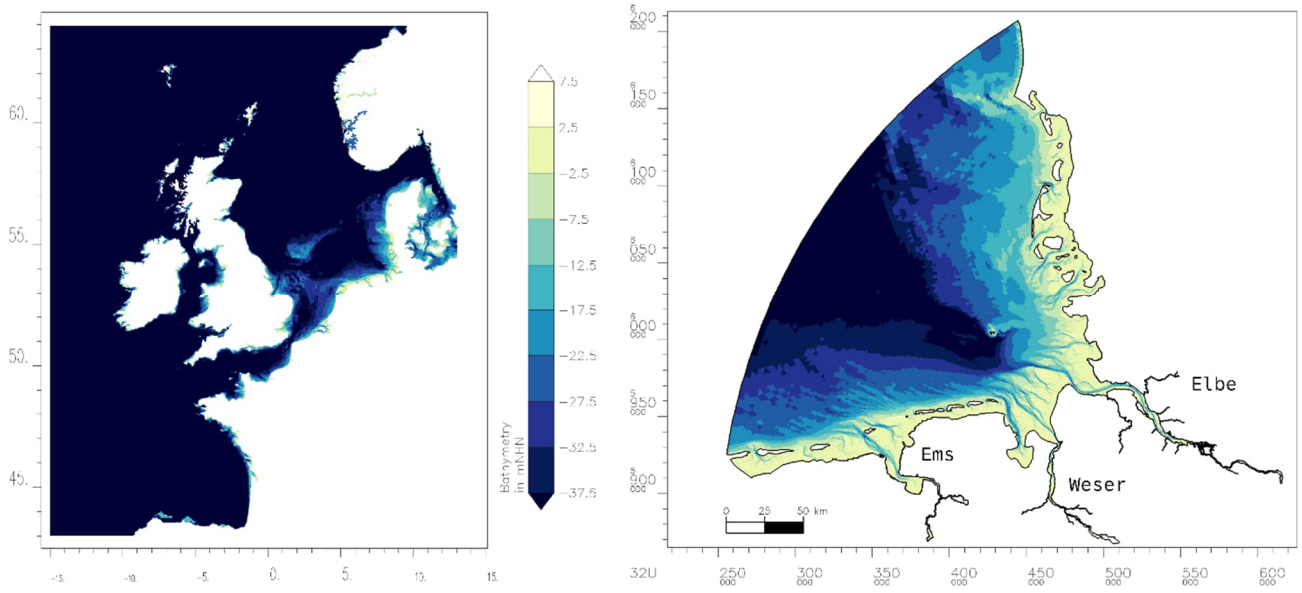

Figure 1: Model domain and bathymetry in m NHN (German vertical datum) of the *DCSMv6FM* model (left) in WGS 84 and of the German Bight model (right) in UTM zone 32N

Since the focus of our study is on the Elbe estuary, a brief validation of the model in this specific region is presented below. Further analysis on model performance can be found in Rasquin et al. (2020). To compare the simulation results with

https://doi.org/10.5194/egusphere-2023-1288
Preprint. Discussion started: 22 June 2023

observations, we simulated seven spring-neap-cycles between January and April 2013 with measured river discharge provided by the Federal Waterways and Shipping Agency (WSV, 2022). Figure 2 shows a visual comparison between the simulation result and the observation of the water level at the stations Cuxhaven (mouth of the estuary) and St. Pauli (close to port of Hamburg) for a short period of time. It can be seen that phase and shape of the vertical tide is well reproduced by the model, but tidal low water is slightly higher in the simulation results compared to the observations.

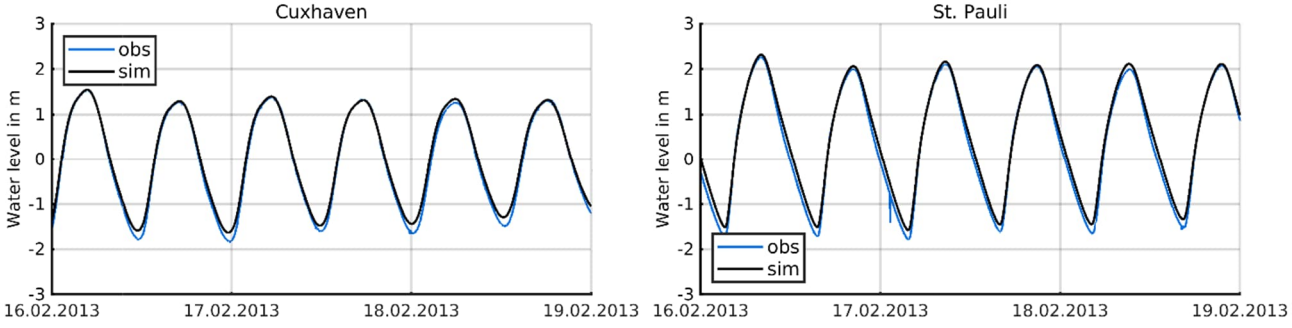

Figure 2: Water level from simulation result (black) and observation (blue) at Cuxhaven and St. Pauli

Figure 3 shows the mean tidal range (*TR*) and mean tidal mean water level (*MW*) along the estuary for the seven spring-neap-cycles, calculated for both the simulation results and observational data at stations along the estuary (WSV, 2022). It shows, that the model is able to reproduce the characteristic development of *TR* along the Elbe estuary, with a strong increase starting around km 60, a maximum reached around km 115 and a decrease further upstream. As a result of the too high tidal low water, *TR* is underestimated by 10-20 cm and *MW* water is overestimated by the model by around 10 cm.

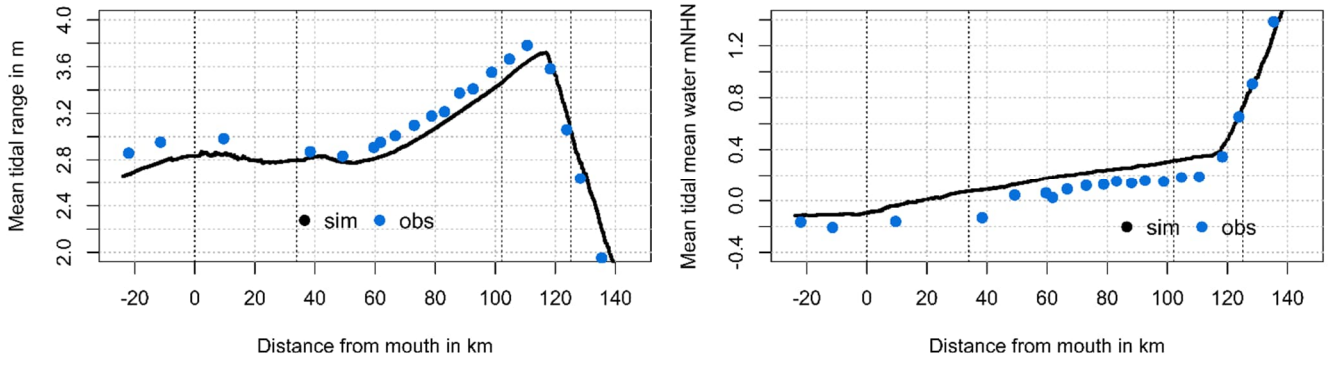

Figure 3: TR (left) and MW (right) above mNHN (meters above the German datum) averaged over 7 spring-neap-cycles in January 2013 to April 2013 along the Elbe estuary calculated from observations (blue) and from the simulation results (black)

https://doi.org/10.5194/egusphere-2023-1288
Preprint. Discussion started: 22 June 2023

2.2 Simulated Scenarios

To investigate the effect of *SLR* and potential corresponding tidal flat growth, several scenarios are simulated and analysed. Two *SLR*-scenarios of 55 and 110 cm were simulated by adding *SLR* at the open boundary of the German Bight model. According to the IPCC 6th Assessment Report (AR6), mean global *SLR* in 2100 compared to the reference period 1995–2014 will be in a likely range of 0.43 to 1.01 m for the intermediate to high-emission-scenarios (SSP2-4.5, SSP3-7.0 and SSP5-8.5) (Fox-Kemper et al., 2021). Our selected *SLR*-scenarios are close to the median of the intermediate scenario and close to the upper range of the high-emission scenario for 2100. Projected values for regional *SLR* in the south-eastern North sea region (Delfzijl, Cuxhaven, Esbjerg) are within a range of ±20 cm of the median of the projected global mean *SLR* until 2100 (Fox-Kemper et al., 2021; Garner et al., 2021).

As mentioned in the introduction, it is uncertain and difficult to quantify to which amount tidal flats in the German Bight will be able to keep up with future accelerated *SLR*. The amount of tidal flat accretion can strongly differ between the tidal basins of the German Bight and is not only dependent on future *SLR* acceleration and magnitude, but also on sediment availability and meteorological conditions. To gain a better understanding of the possible effects of potential *SLR* and tidal flat growth scenarios in the Elbe estuary, we analyse a range of 0%, 50% and 100% tidal flat growth with *SLR*. In these scenarios tidal flat areas in the entire model domain are uniformly elevated by a certain amount, which is a highly simplified assumption.

Table 1: Simulated scenarios

scenario	SLR	Tidal flat elevation
ref	-	-
slr55t0	+55 cm	-
slr55t55	+55 cm	+55 cm Scenario A
slr55t55e	+55 cm	+55 cm Scenario B
slr110t0	+110 cm	-
slr110t55	+110 cm	+55 cm Scenario A
slr110t110	+110 cm	+110 cm Scenario A
slr110t55e	+110 cm	+55 cm Scenario B
slr110t110e	+110 cm	+110 cm Scenario B

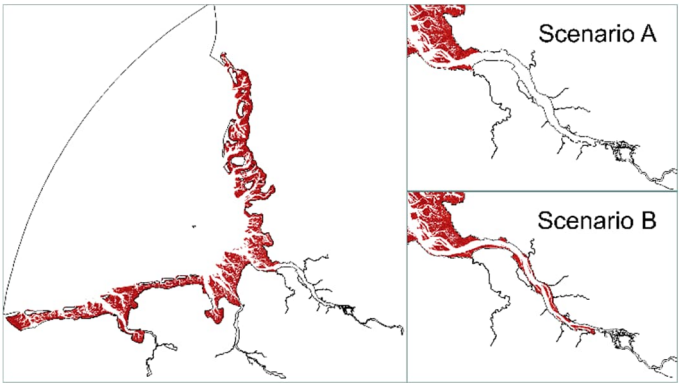

Figure 4: Areas of tidal flat elevation in the model domain

The scenarios with tidal flat growth are further differentiated by firstly elevating tidal flats in the German Bight and in the mouth section of Elbe estuary (scenario A) and secondly elevating tidal flats in the German Bight, the mouth section and also the lower section of the estuary (scenario B) (see Figure 4). This differentiation inside the estuary is done to gain a better understanding of the estuarine system in the context of *SLR* and tidal flat elevation. Table 1 summarises the scenarios simulated with the German Bight model.

https://doi.org/10.5194/egusphere-2023-1288
Preprint. Discussion started: 22 June 2023

2.3 Analysis of Simulation Results

2.3.1 Spatial Decomposition and Definition

Mean tidal parameters are analysed and visualised along the profile of the estuary. The profile is displayed in Figure 5, it starts seawards of the mouth of the estuary and runs upstream along the fairway, along the northern branch until the weir in Geesthacht. For the analysis of the geometric parameters the estuary is divided into 71 control volumes (Figure 5). The control volumes and therefore the analysed geometric parameters do not cover the full length of the estuary profile, as a clear definition of the boundaries is not possible in the outer section of the estuary. However, the tidal parameters are analysed and displayed along the entire profile, even in the outer section. For better comparison between the tidal parameters along the profile and the geometric parameters derived for the control volumes, the zero position of the x-axis in the figures showing results along the estuary is set at the most seaward control volume boundary of the profile. Furthermore, the estuary is roughly divided into five sections, which are displayed in Figure 5 and named (from west to east): outer section, mouth section, lower section, Hamburg section and upper section.

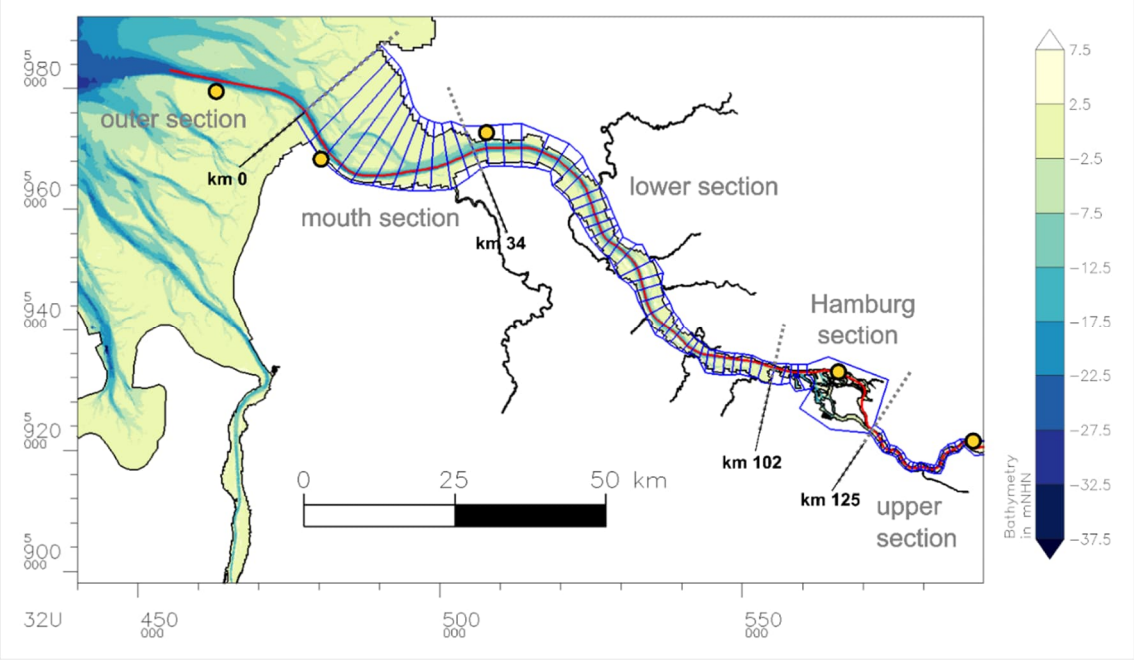

Figure 5: Model excerpt of the Elbe estuary with a display of the profile along the estuary (red) and a subdivision into 5 sections (grey) and 71 control volumes (blue) which are used for the analysis of the simulation results. The yellow markers represent the following locations from left to right: Scharhörn, Cuxhaven, Brunsbüttel, St. Pauli (Hamburg Harbour) and Geesthacht

https://doi.org/10.5194/egusphere-2023-1288
Preprint. Discussion started: 22 June 2023

2.3.2 Tidal and geometric Parameters

The results of the hydrodynamic-numerical simulation are analysed by calculating characteristic parameters of the vertical tide for the domain of the Elbe estuary. All parameters are analysed for one spring-neap cycle in July 2013, simulated with a constant discharge of 600m³/s. Mean tidal parameters of the spring-neap cycle are analysed and visualised along the profile of the estuary displayed in Figure 5. This study mainly focuses on the changes in mean tidal range (*TR*). *TR* is a central parameter in the estuary for characterising tidal dynamics, as it is closely linked to other tidal parameters (e.g. low water (*LW*), high water (*HW*)) which are relevant for navigation, drainage into the estuary and dimensioning of hydraulic structures.

To derive explanatory approaches for the changes of *TR*, changes of estuarine geometry are analysed. The geometric parameters are derived by analysing values for the 71 control volumes/areas along the estuary which are displayed in Figure 5. In the following the three geometric parameters studied will be introduced: convergence length (L_a), mean hydraulic depth (h) and relative intertidal area (φS_{INT}). The geometry of an estuary influences tidal dynamics in an estuary in several ways. As our focus is *TR*, we shortly discuss the potential influence of these three geometric parameters on *TR* in an estuary.

2.3.3 Convergence Length

Background

Upstream convergence of an estuary can cause upstream amplification of tidal waves. This phenomenon is also denoted as 'wave shoaling' or 'wave funneling' (van Rijn, 2011). The tidal wave amplification due to gradual change of width and depth of a system can be explained with the wave energy flux equation, as it is done in Green's Law 1837 (van Rijn, 2011):

Eq. (1):

$$F = 0.125\rho g b H^2 c = Ec, \quad (1)$$

Where F is the energy flux per unit time (wave period) of a progressive sinusoidal wave being equal to E the energy of the wave per unit length of the wave times $c=(gh)^{0.5}$ the wave propagation celerity in shallow water. With H being the tidal wave height (tidal range), b the width of the channel, h the water depth, ρ water density and g gravitational acceleration. According to Greens Law, when the tidal wave is assumed to be a progressive sinusoidal wave in a system without reflection and energy loss due to friction, energy flux is constant and it follows that tidal amplitude varies as $b^{-1/2} h^{-1/4}$ with the channel width (b) of the momentum conveying stream and the depth (h) below a mean tidal water level (Jay, 1991). In an estuary containing a channel and tidal flats, the amplitude varies as $b^{-1/4} b_T^{-1/4} h^{-1/4}$ with b_T being the width at mean water level (Jay, 1991). Based on these considerations, a gradual upstream decrease of cross-sectional-flow area A ($A=hb$) can cause an increase in tidal amplitude and therefore *TR* and an increase of A can cause a decrease of *TR* accordingly.

Analysis of convergence length

A funnel shaped geometry with decreasing width and depth in upstream direction is typical for most alluvial estuaries (van Rijn, 2011). A schematic plan view of a funnel shaped estuary is shown in Figure 6. A mathematical way to represent the shape of an estuary, which has been widely used in many studies (Gisen, 2015), is an exponential function in the form of:

https://doi.org/10.5194/egusphere-2023-1288
Preprint. Discussion started: 22 June 2023

Eq. (2):

$$A = A_0 e^{-\frac{x}{L_a}}, \quad (2)$$

Where A is the cross-sectional-area, A_0 is the cross-sectional area at x=0 (mouth of the estuary), x is the distance from the mouth of the estuary in upstream direction along the estuary axis and L_a is defined as convergence length (the distance from the mouth at which the tangent through the point (0, A_0) intersects with the x-axis) (Savenije, 2012). The parameter L_a describes the rate of the decrease of cross-sectional area in upstream direction. When comparing the convergence length between different estuaries or between different scenarios of the same estuary, a smaller value of L_a indicates a stronger convergence. It should be noted, that some studies use the convergence length of width, and sometime depth, instead of the convergence length of cross-sectional-area (A), to describe the shape of an estuary. Furthermore, several studies do not calculate only one convergence length for an entire estuary, but divide estuaries into sections with distinct convergence lengths. However, we calculate only one convergence length (L_a) for the entire estuary to analyse possible changes of convergence for the entire system. We analyse L_a for each simulated scenario by fitting the exponential function of Eq. (2) to the data of mean cross-sectional-flow-area at the control volume boundaries along the estuary derived by analysis of the simulation results. The mean cross-sectional-flow-area is derived by averaging the mean cross-sectional-flow-area of each tide over the spring-neap-cycle. The exponential function is fitted with a weighted multiple non-linear-least-square regression using the gauss-newton-algorithm. The regression is performed with the nls-toolbox of the R-project (Baty et al., 2015). A multiple regression is necessary to analyse, whether the convergence lengths of the different scenarios are significantly differing. A weighted regression is conducted to reduce the effect of uneven data distribution along the x-axis due to unevenly sized control volumes.

2.3.4 Mean hydraulic Depth

Background

Water depth influences the propagation speed of a tidal wave c in shallow water in the form of $c=(gh)^{0.5}$. According to the wave energy flux equation mentioned above (Eq. (1)), an increase in water depth can therefore increase wave propagation speed and decrease *TR*, if all other parameters remain constant. However, this would be a simplified assumption, as it excludes bottom friction and other shallow water effects which become increasingly important closer to the coast, when tidal amplitude (a) is less small than water depth (h). Energy dissipation due to work done by bed shear stress causes damping of the wave (decrease of *TR*). Water depth in an estuary therefore affects frictional damping of a tidal wave due to energy dissipation which scales by the cube of current velocity over depth (U^3/h) (Simpson and Hunter, 1974; Garrett et al., 1978). Therefore, increased mean water depth in the estuary can have an increasing effect on *TR* by reducing frictional damping of the tidal wave and vice versa. Furthermore, a change in mean water depth can also change *TR* by pushing the system closer to or away from resonance (Talke and Jay, 2020).

https://doi.org/10.5194/egusphere-2023-1288
Preprint. Discussion started: 22 June 2023

Analysis of mean hydraulic depth

The depth over an estuary cross-section (see Figure 6) can be highly variable due to deep channels and shallow intertidal areas. Mean hydraulic depth of an estuary can be defined and calculated in several ways, as discussed by Zhou et al. (2018). Many studies with simplified models assume only the channel as flow-conveying cross-section, excluding intertidal area. Therefore, mean hydraulic depth can be defined including or excluding intertidal area, which has strong influence on the resulting mean hydraulic depth. Two different definitions, which include (h_t) and exclude (h_c) intertidal area into the calculation of mean hydraulic depth are:

Eq. (3):

$$h_t = \frac{V_{MW}}{S_{MW}}, \quad (3)$$

and

Eq. (4):

$$h_c = \frac{V_{LW}}{S_{LW}} + (MW - LW), \quad (4)$$

With V_{MW}, S_{MW}, V_{LW} and S_{LW} being the volume (V) and surface area (S) at mean water level (MW) and mean low water level (LW) (see Figure 6)). We calculate the mean hydraulic depth in each control volume and section for each scenario by using the volume and wetted surface area of the control volumes from the simulation results. Mean hydraulic depth is calculated according to Eq. (3) for the entire cross-section (h_t) and according to Eq. (4) for the channel part of the cross-section only (h_c). The mean volume (V) and wetted surface area (S) at MW and LW is derived by averaging over the spring-neap-cycle.

2.3.5 Relative intertidal Area

Background

Intertidal area is approximately the area of the tidal flats, between tidal low water (LW) and tidal high water (HW), which is periodically wetting and drying. Along-estuary transport of mass and momentum over tidal flats is often assumed to be negligible (Friedrichs, 2010). Tidal flats mainly store water instead of transporting momentum along the estuary (Aubrey and Speer, 1985). Momentum is lost as water flows onto the tidal flats with rising tide and decelerates because of strong friction, and also at the falling tide, as water with zero momentum returns to the momentum carrying channel and must be accelerated (Jay, 1991). Therefore, a loss of intertidal area causes an increase in tidal amplitudes and an increase of intertidal area causes decrease in tidal amplitude (Jay, 1991). According to Song et al. (2013) tidal flats effect tidal energy budget by storage and dissipation, while the former can be more significant than the latter. Based on these considerations an increase of rel. intertidal area (φS_{INT}) can cause a decrease of TR and vice versa.

Analysis of relative intertidal area

A tidal basin or an estuary can be roughly divided into subtidal (S_{LW}) and intertidal area (S_{INT}) (Figure 6). Intertidal area (S_{INT}) is hereby defined as the difference between wetted surface area at mean high water and wetted surface area at mean low water:

https://doi.org/10.5194/egusphere-2023-1288
Preprint. Discussion started: 22 June 2023

Eq. (5):

$$S_{INT} = S_{HW} - S_{LW}, \quad (5)$$

Relative intertidal area (ϱS_{LW}) can be defined as the ratio between S_{INT} and S_{HW}:

Eq. (6):

$$\varrho S_{INT} = \frac{S_{INT}}{S_{HW}} = \frac{S_{HW} - S_{LW}}{S_{HW}}, \quad (6)$$

Different ratios are commonly used to describe the cross-sectional geometry can be often converted into each other and are in detail discussed by Zhou et al. (2018). We define relative intertidal area as the ratio between intertidal area and wet surface area at mean high water (ϱS_{INT}) (Eq. (6)). According to Eq. (6) we calculate relative intertidal area for each control volume and section for each scenario. Mean wetted surface area at *HW* and *LW* is derived from the simulation results for each control volume and averaged over the spring-neap-cycle.

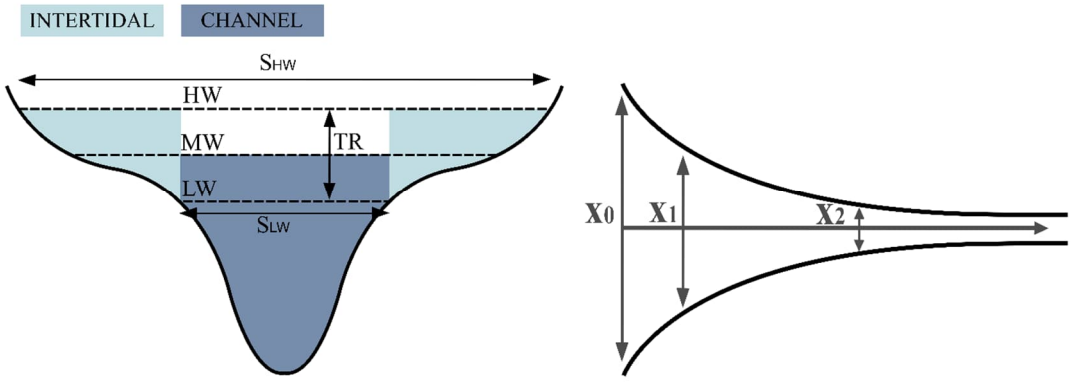

Figure 6: a) schematic cross-section with channel and intertidal volume, high water (*HW*), mean water level (*MW*) and low water (*LW*), tidal range (*TR*) and surface area at *HW* and *LW* (S_{HW} and S_{LW}); b) schematic plan view of a funnel shaped estuary

3 Results

3.1 Tidal Range along the Estuary

In Figure 7 tidal range (*TR)* is visualised for the different simulated scenarios along the profile of the estuary. Other parameters of the vertical tide (high water (*HW),* low water *(LW),* mean water *(MW)*) can be found in the appendix (Figure A1). Hereinafter we focus on the results of the scenarios with 110 cm *SLR* to gain a better system understanding. The scenarios with *SLR* of 55 cm are not visualised and analysed in detail. As apparent in Figure 7, mean tidal range (*TR*) in the Elbe estuary increases in upstream direction, reaches a maximum in the Hamburg section and decreases subsequently. The simulation result for the scenario with sea level rise of 110 cm (*slr110t0*) reveals increased tidal range (*TR*) due to decreased *LW* and increased *HW* relative to the applied sea level rise of 110 cm. *TR* is increased by up to around 15 cm in the mouth section and by around 10 cm in the lower section. Upstream of the Hamburg section, the increase of *TR* intensifies, mainly due to a lowered *LW*. In the case that tidal flats are elevated by 50% with *SLR* (*slr110t55*), no notable changes in *TR* are visible compared to scenario

https://doi.org/10.5194/egusphere-2023-1288
Preprint. Discussion started: 22 June 2023

slr110t0. If, however, tidal flats in the German Bight and the mouth section of the estuary are fully (100%) elevated with sea level rise (*slr110t110*), *TR* is damped relative to scenario *slr110t0*. In contrary, an additional elevation of tidal flats in the entire Elbe estuary (*slr110t110e*) strongly increases *TR* relative to scenario *slr110t0*, especially in the lower section.

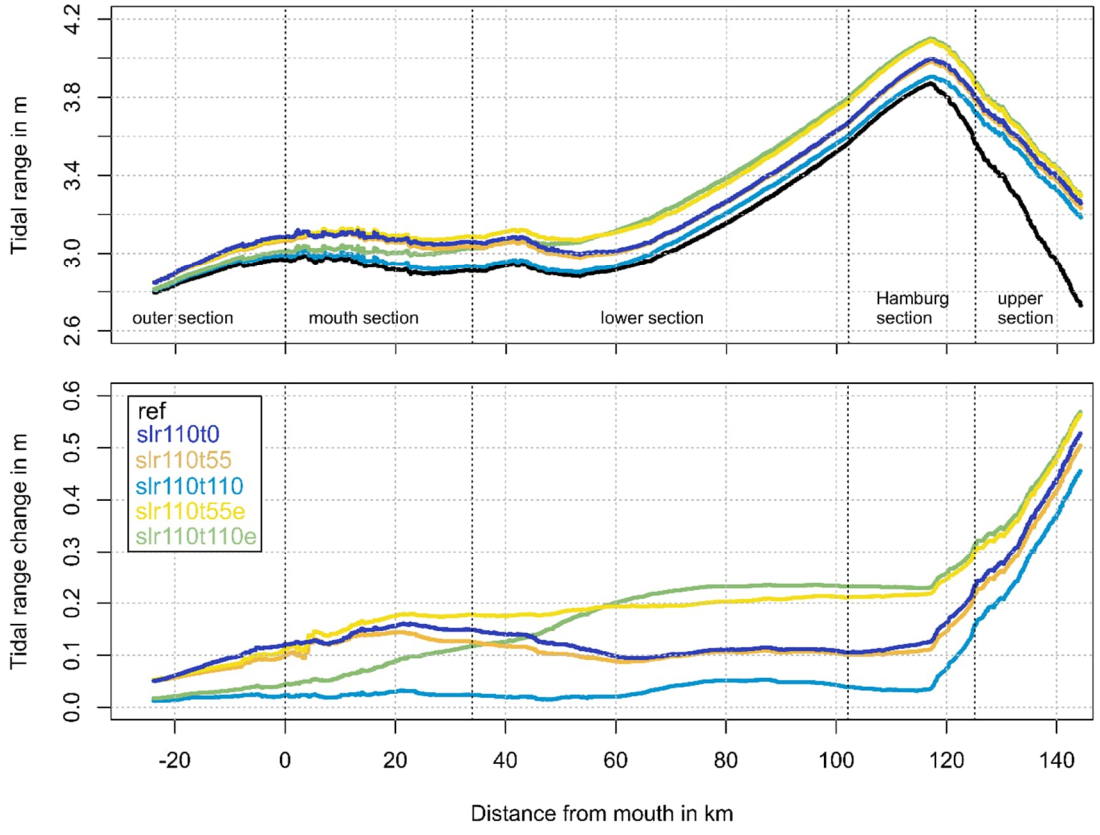

Figure 7: *TR* in m (top) and change in *TR* relative to reference condition in m (bottom) along the estuary profile analysed for a spring-neap cycle for scenario *ref* (black), *slr110t0* (dark blue), *slr110t55* (orange), *slr110t110* (light blue), *slr110t55e* (yellow), *slr110t110e* (green)

For all scenarios, the maximum value of *TR* along the estuary is reached in the Hamburg section. Table 2 lists the changes in max. *TR* relative to reference condition (max. *TR* = 3.87 m) for all simulated scenarios.

https://doi.org/10.5194/egusphere-2023-1288
Preprint. Discussion started: 22 June 2023

345

Table 2: Change in max. TR relative to reference condition

Scenario	*SLR*	Tidal flat elevation	Change in max. *TR*	Change in max. *TR* relative to *SLR*
slr55t0- ref	+55 cm	-	+ 6.5 cm	11.9 %
slr55t55- ref	+55 cm	+55 cm scenario A	+ 4.5 cm	8.1 %
slr55t55e- ref	+55 cm	+55 cm scenario B	+ 14 cm	25.5 %
slr110t0- ref	+110 cm	-	+ 12.5 cm	11.4 %
Slr110t55- ref	+110 cm	+55 cm scenario A	+ 11.1 cm	10.1 %
slr110t110- ref	+110 cm	+110 cm scenario A	+ 3.5 cm	3.2 %
Slr110t55e- ref	+110 cm	+55 cm scenario B	+ 21.8 cm	19.8 %
slr110t110e- ref	+110 cm	+110 cm scenario B	+ 23 cm	20.9%

350 The analysis shows changes of *TR* in the estuary which strongly differ between the different simulated scenarios. In some tidal flat growth scenarios *TR* is increased relative to sole *SLR* without topographic changes, while in other scenarios it is decreased. At first glance and without further investigation, a simple explanation for these changes is not apparent. To derive explanatory approaches for the changes of *TR*, changes of estuarine geometry for some scenarios are analysed and displayed hereinafter.

3.2 Changes of estuarine Geometry

355 **63.2.1 Convergence Length of cross-sectional-flow-Area**

Figure 8 shows the mean cross-sectional flow area (*A*) at the control-volume boundaries along the estuary. For better readability, the results of scenarios *slr110t55* and *slr110t55e* are not shown in the figure. The displayed flow area is the mean area through which the water flux of a tide flows, averaged over one spring-neap-cycle. The results show a typical upstream decrease of *A* in all scenarios. As a consequence of sea level rise (scenario *slr110t0*), *A* increases along the estuary relative to
360 the reference scenario. Elevated tidal flats in the mouth of the estuary (*slr110t110* and *slr110t55*) cause a decrease of *A* in this section compared to *slr110t0*. Additional elevated flats in the lower section of the Elbe estuary (*slr110t110e* and *slr110t55e*) slightly decrease *A* in this section accordingly.

https://doi.org/10.5194/egusphere-2023-1288
Preprint. Discussion started: 22 June 2023

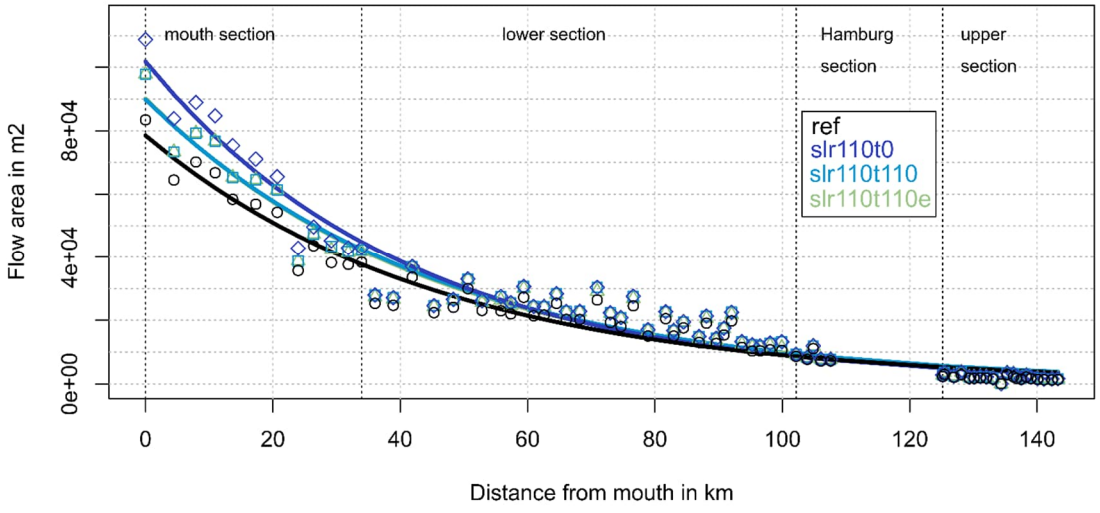

Figure 8: Cross-sectional flow area *A* analysed for each control volume boundary along the estuary profile (markers) and fitted regression model (lines) for scenario *ref* (black), *slr110t0* (dark blue, rhombuses), *slr110t110* (light blue, squares), *slr110t110e* (green, triangles). (The results of scenarios *slr110t55* and *slr110t55e* are not shown in the figure for better readability)

To access the rate at which cross-sectional-flow-area of an estuary decreases in upstream direction, the geometric parameter convergence length (L_a) is calculated by fitting an exponential function (Eq. (2)) to the data sets (see 2.3.3). To evaluate, if the convergence length significantly changes between two scenarios a multiple regression is performed. The results of the weighted multiple non-linear least square regression for the reference condition and all *slr110* scenarios are displayed in Table 3.

Table 3: Results of the multiple non-linear-least-square regression for the cross-sectional-flow-area along the estuary fitted to Eq. (2). Results with a p-value > 0.1 are considered not significant (n.s.).

Scenario	A_0 in m^2	p-value of A_0	L_a in km	p-value of L_a
ref	78.5 x10^3	<0.001	46.3	<0.001
slr110t0-ref	+23.3 x10^3	<0.001	-4.9	0.026
slr110t0	101.7 x10^3	<0.001	41.4	<0.001
slr110t110 - slr110t0	-11.9 x10^3	<0.001	+4.0	0.070
slr110t110e - slr110t0	-11.6 x10^3	<0.001	+3.3 (n.s.)	0.130 (n.s.)
slr110t55- slr110t0	-4.8 x10^3 (n.s.)	0.134 (n.s.)	+1.3 (n.s.)	0.519 (n.s.)
slr110t55e- slr110t0	-4.6 x10^3 (n.s.)	0.148 (n.s.)	+1.0 (n.s.)	0.642 (n.s.)

The derived convergence length (L_a) of the Elbe estuary for the mean cross-sectional-flow area (A) of the spring-neap-cycle is 46.3 km in the reference condition and 41.4 km in the scenario *slr110t0*. Depending on the p-value for the difference of L_a between two scenarios, the null hypothesis of no change in convergence length L_a can, or cannot be rejected. For the difference between L_a of scenario *slr110t0* and the reference condition, the null hypothesis can be rejected with a significance level of

https://doi.org/10.5194/egusphere-2023-1288
Preprint. Discussion started: 22 June 2023

α=005. The detected significant decrease of L_a indicates a stronger convergence, hence a stronger rate of decrease of A in upstream direction due to *SLR* of 110 cm. For the difference of convergence length between scenario *slr110t110* and *slr110t0* the null hypothesis can be rejected with a significance level of α=0.1, which indicates, that in scenario *slr110t110*, convergence is significantly weakened compared to scenario *slr110t0*. For the other scenarios no significant change of convergence length relative to scenario *slr110t0* can be detected with the applied method and a significance level of α≤0.1. These results are marked with *n.s.* (not significant).

3.2.2 Mean hydraulic Depth

As mentioned in 2.3.4 mean hydraulic depth for each section and for each scenario is calculated in two different ways, including (h_t) and excluding (h_c) intertidal area into the calculation of hydraulic depth. The results of mean hydraulic depth for reference condition and each *slr110* scenario and section are displayed in Table 4. Figure 9 displays the relative change of mean hydraulic depth of the scenarios *slr110t0*, *slr110t110* and *slr110t110e* relative to the reference scenario (*ref*) for each control volume and section.

Table 4: Mean hydraulic depth of the entire cross-section (h_t) and of the channel (h_c) in the Elbe estuary in m

Scenario	mouth section		lower section		Hamburg section		upper section		entire estuary	
	h_t	h_c	h_t	h_c	h_t	h_c	h_c	h_t	h_t	h_c
ref	5.7	8.2	8.8	10.6	9.6	10.4	4.7	5.2	7.0	9.2
slr110t0	5.7	7.7	8.7	10.5	10.2	11.0	5.1	5.9	6.9	9.0
slr110t110	6.3	8.7	8.7	10.5	10.2	11.0	5.1	6.0	7.4	9.6
slr110t110e	6.4	8.8	9.6	11.1	10.2	11.0	5.1	6.0	7.7	9.9
slr110t55	6.0	8.3	8.7	10.5	10.2	11.0	5.1	6.0	7.2	9.4
slr110t55e	6.0	8.4	9.1	10.9	10.2	11.0	5.1	6.0	7.3	9.5

https://doi.org/10.5194/egusphere-2023-1288
Preprint. Discussion started: 22 June 2023

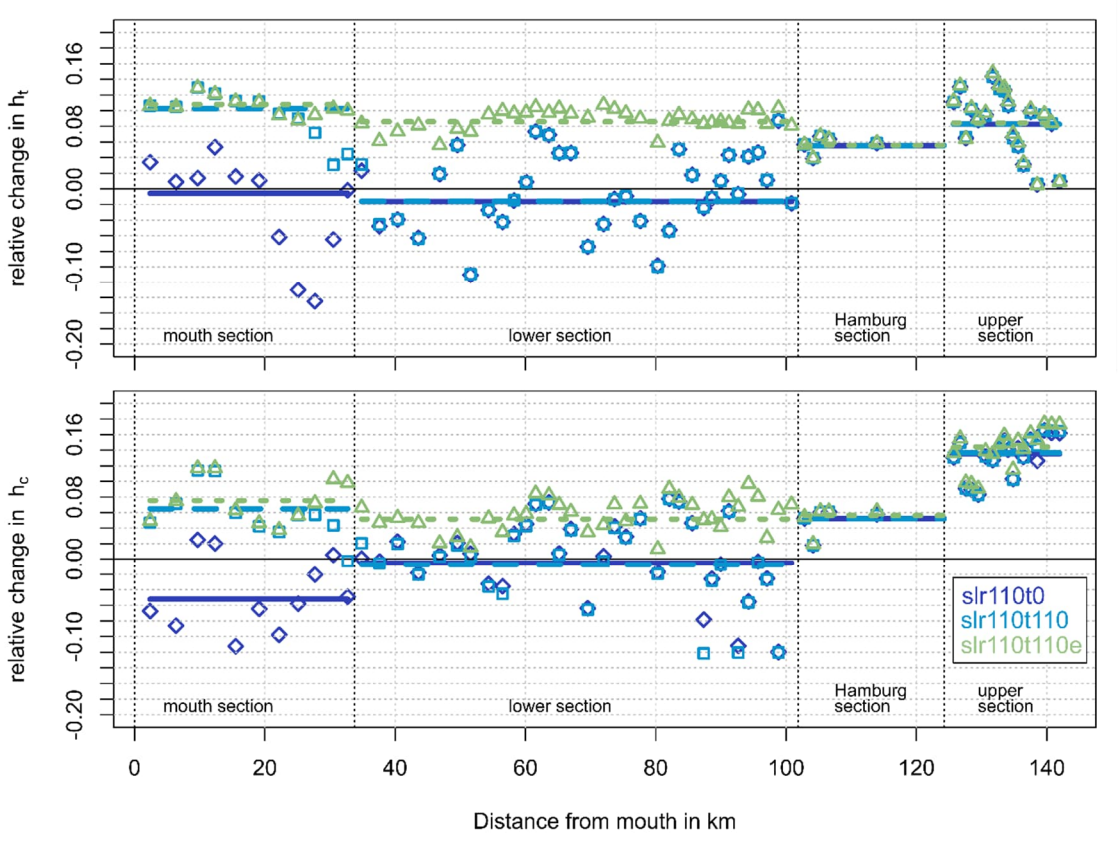

395 **Figure 9: Relative change of mean hydraulic depth (h_t top and h_c bottom) in each control volume and each section relative to reference condition for scenario *slr110t0* (dark blue rhombuses), *slr110t110* (light blue squares), *slr110t110e* (green triangles). (The results of scenarios *slr110t55* and *slr110t55e* are not shown in the figure for better readability)**

The results indicate, that *SLR* of 110 cm (*slr110t0*) does not in general cause an increase in mean hydraulic depth along the
400 estuary. In contrary, h_t and h_c show even a decrease in some parts of the estuary. Averaged over sections, *slr110t0* causes almost no changes of h_t in the mouth section, a slight decrease in the lower section and an increase in the Hamburg section and the upper section. In regions where tidal flats are elevated (*slr11t110*: mouth section; *slr110t110e*: mouth section as well as lower section) mean hydraulic depth increases due to *SLR*. The changes of h_c are qualitatively similar to h_t. Mean hydraulic depth excluding intertidal area (h_c) shows a stronger decrease due to sole *SLR* and in the mouth section.

https://doi.org/10.5194/egusphere-2023-1288
Preprint. Discussion started: 22 June 2023

3.2.3 Relative intertidal Area

Mean relative intertidal area ($\varnothing S_{INT}$) for each section along the estuary is displayed in Table 5 and Figure 10. Figure 10 additionally visualises the relative changes in $\varnothing S_{INT}$ compared to the reference condition. In general, relative intertidal area is greatest in the mouth section and decreases along the estuary to the Hamburg section.

Table 5: $\varnothing S_{INT}$ in the Elbe estuary

Scenario	mouth section	lower section	Hamburg section	upper section	entire estuary
ref	0.49	0.28	0.16	0.25	0.40
slr110t0	0.41	0.31	0.16	0.34	0.37
slr110t110	0.47	0.31	0.16	0.34	0.39
slr110t110e	0.47	0.25	0.16	0.35	0.38
slr110t55	0.46	0.31	0.16	0.34	0.39
slr110t55e	0.46	0.30	0.16	0.34	0.39

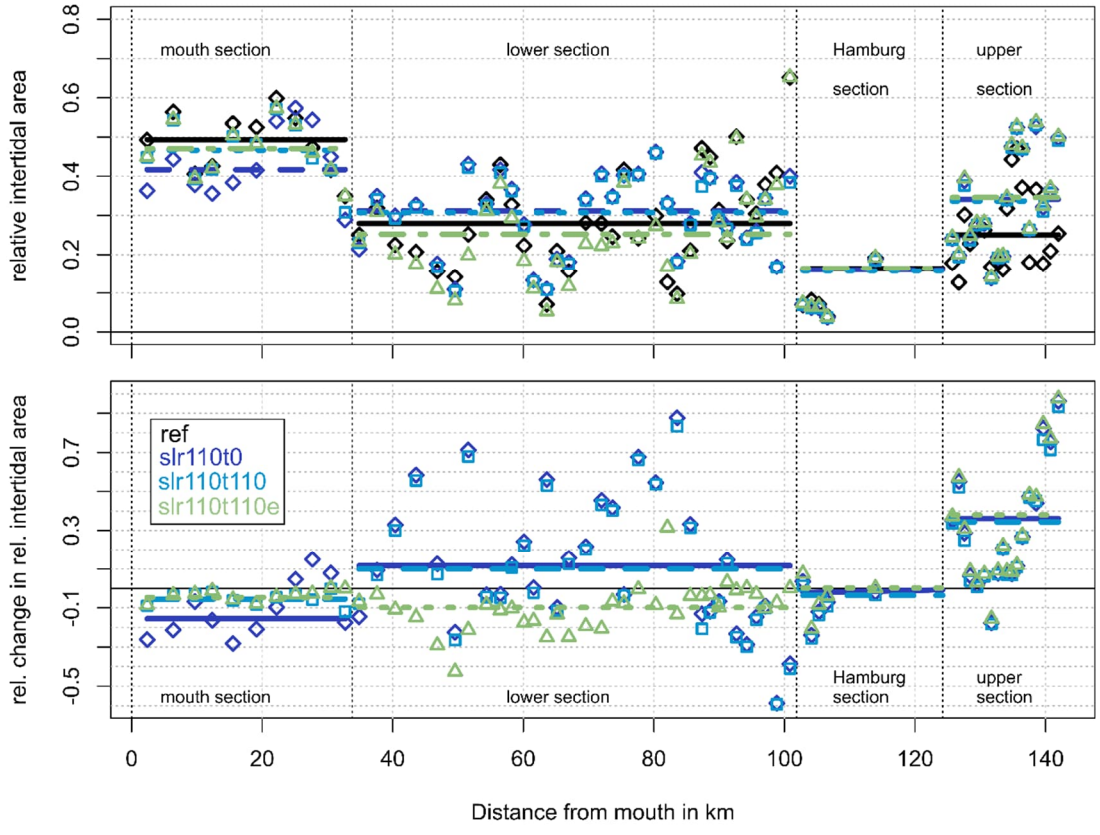

Figure 10: Relative intertidal area (top) and relative change in relative intertidal area (bottom) in each control volume and section along the estuary for scenario ref (black), *slr110t0* (dark blue rhombuses), *slr110t110* (light blue squares), *slr110t110e* (green triangles). (The results of scenarios *slr110t55* and *slr110t55e* are not shown in the figure for better readability)

https://doi.org/10.5194/egusphere-2023-1288
Preprint. Discussion started: 22 June 2023

Due to *SLR* of 110 cm (*slr110t0*) ϱS_{INT} decreases by about 15% in the mouth section, increases by about 10% in the lower section, remains unchanged in the Hamburg section and strongly increases in the upper section. A tidal flat elevation counteracts the changes of *SLR* in the sections where tidal flats are elevated (mouth section and lower section). In the Hamburg section and the upper section, where no tidal flats are elevated, tidal flat elevation causes almost no changes in ϱS_{INT} relative to *slr110t0*.

4 Discussion

4.1 Objectives and Limitations

Using a three-dimensional hydrodynamic-numerical model of the German Bight, we investigate the effect of potential future *SLR* and tidal flat growth scenarios on tidal dynamics in the Elbe estuary. As it is difficult to predict the future development of tidal flats in the German Bight in the context of accelerated *SLR*, we simulate simplified scenarios with uniformly elevated tidal flats of 0%, 50% and 100% with *SLR*.

The model calculates water level, current velocity and salt transport on an unstructured orthogonal grid. To reduce computational effort the generation of wind waves as well as sediment and heat transport is not included in our model setup. Thus, potential changes in sediment dynamics, e.g. changes in the *ETM* (estuarine turbidity maximum) and their potential effect on tidal dynamics are neglected. Furthermore, our investigation does not include potential future changes in river discharge into the Elbe estuary, as the discharge in the model is kept constant (600 m³/s).

However, the aim of this study is to gain a better system understanding of the Elbe estuary in the context of *SLR* and accompanying topographic changes. We do not attempt to produce realistic projections of future changes. Our focus lies on the changes of the vertical tide in the Elbe estuary, especially tidal range *(TR)*, which is closely linked to other tidal parameters and is relevant for several human activities (e.g. navigation, hydraulic structures).

4.2 Changes in Tidal Range

Our simulation results show, that *SLR* of 55 and 110 cm causes an increase of *TR* in the estuary as *LW* is elevated less than *HW*. Effects of tidal flat elevation with *SLR* on *TR* strongly differ between the simulated scenarios. Tidal flat elevation can have no effect, decrease or increase *TR* relative to sole *SLR*, depending on the location and amount of tidal flat elevation. Tidal flat elevation in the mouth of the estuary can decrease *TR* while tidal flat elevation in the lower section of the estuary increases *TR* relative to sole *SLR*.

As a simple explanation for these various changes of *TR* in the different simulated scenarios is not apparent at first glance, changes of estuarine geometry are analysed for reference condition and all scenarios with 110 cm *SLR* to derive explanatory approaches. As *TR* shows qualitatively similar changes in the scenarios with *SLR* of 55 cm, those are assumingly induced by

https://doi.org/10.5194/egusphere-2023-1288
Preprint. Discussion started: 22 June 2023

similar alterations in estuarine geometry as for a *SLR* of 110 cm. Three geometric parameters were analysed to find indications for the cause of these changes in *TR*: convergence length, mean hydraulic depth and relative intertidal area.

4.3 Changes in Geometry

4.3.1 Convergence Length

Our estimated values for the convergence length (L_a) of the estuary in reference condition is 46.5 km. This value lies in the same order of magnitude of the values estimated by Dronkers (2017) (42 km) and Savenije et al. (2008) (30 km) for the Elbe estuary. Scenario *slr110t0* results in a significant decrease of L_a and therefore a stronger convergence of the Elbe estuary relative to reference condition. In scenario *slr110t110* a weakening of upstream convergence relative to *slr110t0* is detected, which results in a L_a close to reference condition.

A change in L_a is a result of stronger or weaker changes of *A* along the estuary in upstream direction due to regional differences in cross-sectional geometry. As discussed in Friedrichs et al. (1990), change of intertidal storage capacity, cross-sectional-flow-area and channel width due to *SLR* is strongly dependent on the gradient of the estuary banks. Correspondingly, the model results show a stronger increase in cross-sectional-flow-area in the mouth section of the Elbe estuary which contains larger tidal flat areas (meaning low topographic gradient) compared to other sections. It can therefore be assumed, that increased convergence of *A* in upstream direction due to *SLR* is based on the fact that the amount of relative intertidal area in the Elbe estuary is declining in upstream direction (Figure 10).This effect is sketched in Figure 11. Tidal flat elevation seems to significantly counteract this effect in scenario *slr110t110*, but not in the other scenarios.

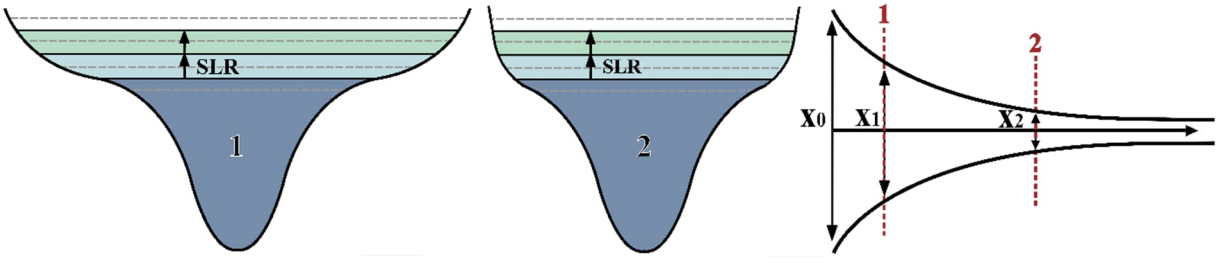

Figure 11: Schematic display of *SLR* in estuary cross-sections (left) and schematic plan view of an estuary (right)

4.3.2 Mean hydraulic Depth

In the reference scenario we derive a mean hydraulic depth averaged over the entire estuary (until the weir in Geesthacht) of 7.0 m for h_t (including intertidal area) and 9.2 m for h_c (excluding intertidal area). In comparison, Savenije et al. (2008) listed a mean depth at *MW* of 7.0 m decreasing upstream to 9.0 m for the Elbe estuary and Dronkers (2005) listed a time-averaged channel depth of 10.0 m for the Elbe estuary. However, it is not clear how these numbers were derived.

Our simulation results for the *SLR* scenarios might be unexpected and counterintuitive, as they show that *SLR* of 110 cm does not in general cause an increase in mean hydraulic depth along the estuary. In contrary, mean hydraulic depth shows no changes

https://doi.org/10.5194/egusphere-2023-1288
Preprint. Discussion started: 22 June 2023

and even a decrease in some parts of the estuary for *slr110t0* relative to the reference scenario. A decrease of h_c due to *SLR* can be explained by shallow areas next to the previous channels becoming part of the now wider channel (Friedrichs et al., 1990) and a decrease of h_t can be in addition explained by shallow previous supratidal areas becoming intertidal areas (see Figure 12). If tidal flats are elevated with *SLR* in the model, they cause a regional increase in mean hydraulic depth relative to *slr110t0* and relative to reference condition in the Elbe estuary. This can be explained by tidal flat elevation counteracting the previously mentioned effect of shallow areas becoming part of the subtidal and intertidal cross-section, which overall results in an increase of mean hydraulic depth due to *SLR* in these scenarios.

4.3.3 Relative intertidal Area

We define relative intertidal area (ςS_{INT}) as the ratio between intertidal area and wet surface area at high water (Sect. 2.3.5). For the reference condition we analyse a mean ςS_{INT} of 0.4 for the entire estuary, which is slightly lower than the value of 0.5 derived by Dronkers (2005) for the Elbe estuary and in the range of 0.412 decreasing upstream to 0 given by Savenije et al. (2008). Note that Dronkers (2005) and Savenije et al. (2008) used a different form (ratio of width at *HW* to width at *LW*) and these numbers are converted for comparability. According to our simulation results, *SLR* of 110 cm causes regionally strongly varying changes of ςS_{INT}, namely a decrease of ςS_{INT} in the mouth section and an increase in the lower section and the upper section of the estuary. Tidal flat elevation counteracts these changes regionally.

Sea level rise can in general cause an increase, decrease, or no change in S_{INT}, depending on the local topographic gradient above *LW* and a potential change in *TR* (see Figure 12). An increase in S_{INT} can be the result of previously supratidal areas (above old *HW*) becoming part of the S_{INT} due to sea level rise (Dronkers, 2005) and/or can be caused by the increase of *TR*. A decrease of S_{INT} can occur in tidal systems which are e.g. restricted by dikes or high gradient topography which can result in larger previously S_{INT} becoming subtidal area (S_{LW}) than previously supratidal area becoming S_{INT} due to *SLR* (Dronkers, 2005) (see Figure 12) and/or can be caused by a decrease of *TR*.

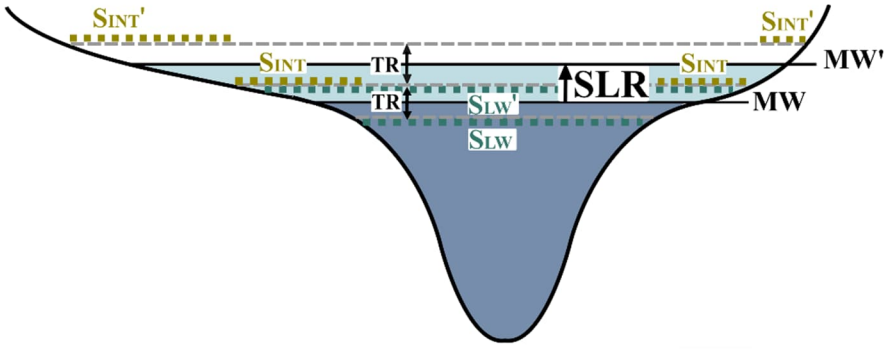

Figure 12: schematic display of *SLR* in estuary cross-sections and its resulting change in intertidal area (S_{INT}) for different topographic gradients between high water (*HW*) and low water (*LW*)

https://doi.org/10.5194/egusphere-2023-1288
Preprint. Discussion started: 22 June 2023

4.4 Explanatory Approaches for the Changes in Tidal Range based on Changes in Geometry

The effects of the previously discussed changes in geometric parameters on tidal dynamics act simultaneously and can therefore counteract, outweigh or enhance each other in the resulting effect on *TR*. However, we want to point out correlations between the detected changes of geometry and *TR* to find explanatory approaches for the latter.

SLR of 110 cm without topographic changes

The simulation results show an increase of *TR* in the estuary in scenario *slr110t0* relative to reference condition. In accordance, analysis of the upstream convergence of cross-sectional-flow-area (*A*) shows a significant increase of convergence in scenario *slr110t0* relative to reference condition. We suspect this is the main reason for the increase in *TR* in *slr110t0*, as gradually converging width and depth causes amplification of a tidal wave according to Green's law (1837) (Sect. 2.3.3). A decrease of $\wp S_{INT}$ is detected in the mouth section and an increase is detected further upstream. Averaged over the entire estuary $\wp S_{INT}$ decreases, which could also contribute to the increase in *TR* (Sect. 2.3.5). Mean hydraulic depth stays approximately unchanged relative to reference condition in the largest part of the estuary. Overall it slightly decreases, thus potentially counteracts the increase of *TR* (Sect. 2.3.4). In the Hamburg section and the upper section an increase of mean hydraulic depth is detected. The hydrodynamics in this upper part of the estuary are not fully dominated by the tide, but also highly influenced by the discharge. Therefore, we assume the strong increase in *TR* in these sections to be caused by an increase of tidal influence relative to discharge-influence.

SLR of 110 cm with tidal flat elevation in scenario A

In scenario *slr110t55* *TR* does not change compared to *slr110t0*. In accordance, analysis of convergence does not show significant changes compared to *slr110t0*. The effect of the detected increase of $\wp S_{INT}$ in the mouth section might be counteracted by the increase of mean hydraulic depth in this section and therefore does not change *TR* relative to *slr110t0*. However, if tidal flats in scenario A are elevated by 100% with *SLR* (*slr110t110*), *TR* decreases relative to *slr110t0* along the entire estuary. In accordance, our analysis shows a significant decrease of convergence in *slr110t110* compared to *slr110t0*, which might be the main reason for *TR* to decrease. An increase of $\wp S_{INT}$ and mean hydraulic depth is detected in the mouth section which might contribute and counteract to the decrease of *TR* respectively.

SLR of 110 cm with tidal flat elevation in scenario B

In the tidal flat elevation scenarios B with tidal flat elevation in the German Bight, the mouth section and the lower section of the estuary (*slr110t55e* and *slr110t110e*), *TR* shows a strong increase relative to scenario *slr110t0*. In these scenarios a significant change in convergence relative to *slr110t0* cannot be detected. A decrease in $\wp S_{INT}$ relative to *slr110t0* is detected in the lower section which might be part of the reason for the increase of *TR*. However, we suspect that the main reason for the increase in *TR* in these scenarios is due to the change in mean hydraulic depth, which increases as tidal flat are elevated. Therefore, compared to the reference condition, both convergence and hydraulic depth are increased in these scenarios, with both changes presumably leading to an increase in *TR*. As mentioned in Sect. 2.3.4, changes in water depth influence frictional damping of a tidal wave due to energy dissipation and can also push a system closer to, or further away from resonance.

https://doi.org/10.5194/egusphere-2023-1288
Preprint. Discussion started: 22 June 2023

Whether the increase in *TR* due to increased mean hydraulic depth is mainly caused by a decrease of frictional damping or by a shift towards resonance needs further investigation.

5 Conclusion and Outlook

The aim of this study is to gain a better system understanding of the Elbe estuary in the context of sea level rise (*SLR)* and accompanying topographic changes. Using a three-dimensional-hydrodynamic-numerical model of the German Bight we investigate the effect of *SLR* and several simplified tidal flat elevation scenarios on tidal dynamics in the Elbe estuary. Due to *SLR* of 55 and 110 cm the simulation results reveal an increase of tidal range (*TR*) in the estuary. The results further show, that potential tidal flat elevation with *SLR* has a notable effect on *TR*, which strongly differs between the scenarios. Potential tidal flat growth can have no effect, decrease or increase *TR* relative to sole *SLR*, depending on the location and amount of tidal flat elevation. Further analysis of the simulation results is conducted for the scenarios with 110 cm *SLR*. We analyse three geometric parameters of the estuary to find indications for the cause of the changes in *TR*: convergence of cross-sectional-flow area, mean hydraulic depth and relative intertidal area.

The results reveal an increase of upstream convergence of cross-sectional-flow-area in the estuary due to sole *SLR* of 110 cm, which is counteracted in the tidal flat growth scenario *slr110t110*, where tidal flats in the mouth of the estuary grow to 100% with SLR. Our analyses suggest that these changes in estuarine convergence might be the main reason for the respective increase and decrease of *TR* in these scenarios. Additionally, we find that sole *SLR* does not cause a general increase of mean hydraulic depth along the estuary, but shows almost no changes or even a decrease in large parts of the estuary. However, if tidal flats are elevated with *SLR*, mean hydraulic depth is increased in the regions of the tidal flat elevation. Therefore, an additional increase of tidal flats in the lower section of the estuary (scenarios *slr110t55e* and *slr110t110e*) causes an increase in mean hydraulic depth in a large part of the estuary, which is likely to be the main reason for the increase in *TR* relative to sole *SLR* in these scenarios.

We are able to use the detected changes in estuarine geometry to find qualitative explanatory approaches for the changes of *TR*. Therefore, the analysis of simplified parameters of estuarine geometry, originally developed in studies with analytical models, has proven useful for understanding and interpreting the results of advanced numerical models. However, to further quantify and separate the influence of the changes of each analysed geometric parameter on *TR*, an analytical model of the estuary could be used with the mentioned geometric parameters as input values. For further generalised understanding, it would be helpful to conduct similar analyses in other estuaries. Therefore, in future studies we plan to carry out similar investigations for other estuaries in the German Bight.

This study focuses on the changes of parameters of the vertical tide, especially *TR* due to *SLR* and potential accompanying tidal flat growth scenarios. Future studies could additionally address the analysis of changes in current velocities, tidal asymmetry and salt intrusion, as they are of concern regarding sediment management and other human activities in and around the estuary as well as biodiversity.

https://doi.org/10.5194/egusphere-2023-1288
Preprint. Discussion started: 22 June 2023

In order to mitigate changes caused by future *SLR* the findings of this study are helpful for the development of adaption measures in the Elbe estuary. The results underline the importance of taking topographic changes into account when analysing the dependence of tidal dynamics in estuaries on future sea level rise, which is necessary, for example, as a basis for adapting infrastructure along the waterway. This study demonstrates that *SLR* and potential corresponding tidal flat elevation scenarios
565 can cause changes in tidal dynamics which are strongly dependent on the individual topography of an estuary and the corresponding change of estuarine geometry.

Appendix

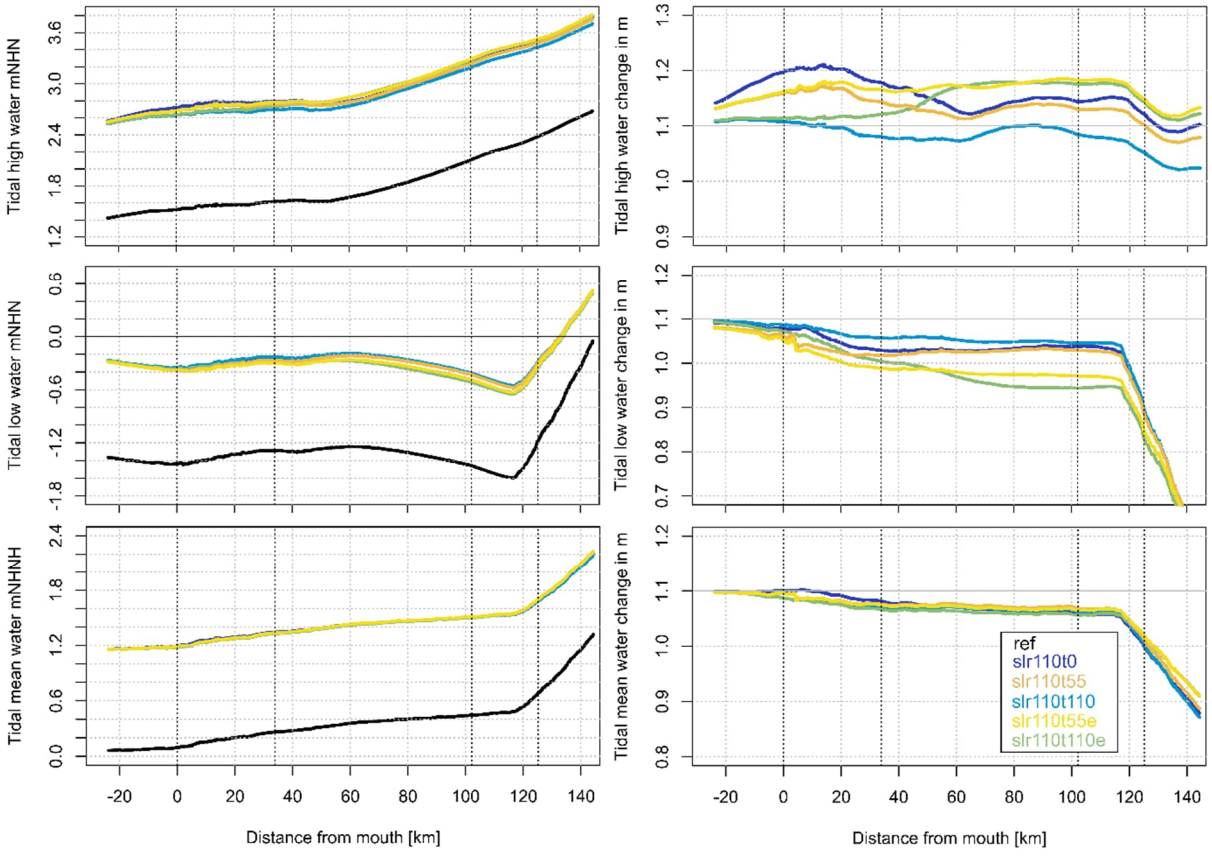

Figure A1: *HW*, *LW* and *MW* relative to mNHN (German vertical Datum) (left) and changes in these parameters relative to reference
570 **condition in m (right) along the estuary profile analysed for a spring-neap cycle for scenario ref (black), *slr110t0* (dark blue), *slr110t55* (orange), *slr110t110* (light blue), *slr110t55e* (yellow), *slr110t110e* (green)**

https://doi.org/10.5194/egusphere-2023-1288
Preprint. Discussion started: 22 June 2023

Data availability

The raw simulation results, as well as the results from the analysis are available, upon request, from the corresponding author. Water level and river discharge measurement data can be accessed from the open data portal of the Federal Waterways and Shipping Administration (WSV, 2022). The *COSMO-REA6* data used for the atmospheric forcing of our model can be accessed from DWD (2022).

Author contributions

TM worked on the simulations, analysis, figures and interpretation. TM wrote the article with contributions from RS. JK, PF and RS were involved as scientific experts, supervised the study and gave input for writing and revision of the paper.

Competing interests

The authors declare that they have no conflict of interest.

Acknowledgements

We thank the German Federal Ministry for Digital and Transport for funding this work as part of the Network of Experts. Furthermore, we thank our co-workers at the Federal Waterways Engineering and Research Institute in Hamburg for their continuous support. Special thanks go to Elisabeth Rudolph, Caroline Rasquin, Ingo Hache, Norbert Winkel and Ralf Fritzsch for their support and inspiring discussions and to Günther Lang for the development of the employed postprocessing tools.

Funding

This study was funded by the German Federal Ministry for Digital and Transport (BMDV) in the context of the BMDV Network of Experts.

References

Aubrey, D. G. and Speer, P. E.: A study of non-linear tidal propagation in shallow inlet/estuarine systems Part I: Observations, Estuarine, Coastal and Shelf Science, 21, 185–205, doi:10.1016/0272-7714(85)90096-4, 1985.

Baty, F., Ritz, C., Charles, S., Brutsche, M., Flandrois, J.-P., and Delignette-Muller, M.-L.: A Toolbox for Nonlinear Regression in R The Package nlstools, J. Stat. Soft., 66, doi:10.18637/jss.v066.i05, 2015.

Becherer, J., Hofstede, J., Gräwe, U., Purkiani, K., Schulz, E., and Burchard, H.: The Wadden Sea in transition - consequences of sea level rise, Ocean Dynamics, 68, 131–151, doi:10.1007/s10236-017-1117-5, 2018.

https://doi.org/10.5194/egusphere-2023-1288
Preprint. Discussion started: 22 June 2023

Benninghoff, M. and Winter, C.: Recent morphologic evolution of the German Wadden Sea, Scientific reports, 9, 9293, doi:10.1038/s41598-019-45683-1, 2019.

Boehlich, M. J. and Strotmann, T.: Das Elbeästuar, Die Küste 87 (2019), Kuratorium für Forschung im Küsteningenieurwesen (KFKI), doi:10.18171/1.087106, 2019.

Bollmeyer, C., Keller, J. D., Ohlwein, C., Wahl, S., Crewell, S., Friederichs, P., Hense, A., Keune, J., Kneifel, S., Pscheidt, I., Redl, S., and Steinke, S.: Towards a high-resolution regional reanalysis for the European CORDEX domain, Q.J.R. Meteorol. Soc., 141, 1–15, doi:10.1002/qj.2486, 2015.

Carrère, L., Lyard, F., Cancet, M., Guillot, A., and Roblou, L.: FES 2012: A New Global Tidal Model Taking Advantage of Nearly 20 Years of Altimetry, Noordwijk, ESA SP, 2013.

Casulli, V.: A high-resolution wetting and drying algorithm for free-surface hydrodynamics, Int. J. Numer. Meth. Fluids, 60, 391–408, doi:10.1002/fld.1896, 2009.

Casulli, V. and Walters, R. A.: An unstructured grid, three-dimensional model based on the shallow water equations, Int. J. Numer. Meth. Fluids, 32, 331–348, 2000.

Dissanayake, D. M. P. K.: Modelling morphological response of large tidal inlet systems to sea level rise: Dissertation submitted in fulfillment of the requirements of the Board for Doctorates of Delft University of Technology and of the Academic Board of the UNESCO-IHE Institute for Water Education for the degree of doctor to be defended in public on Monday, 12 December 2011 at 15:00 hours in Delft, the Netherlands, CRC Press, Taylor & Francis Group, Boca Raton, Fla., 1 online resource (viii, 180, 2012.

Dronkers, J.: Dynamics of coastal systems, Advances series on ocean engineering, 25, WORLD SCIENTIFIC, New Jersey, 519 pp., 2005.

Dronkers, J.: Convergence of estuarine channels, Continental Shelf Research, 144, 120–133, doi:10.1016/j.csr.2017.06.012, 2017.

DWD: OPENDATA: https://opendata.dwd.de/climate_environment/REA/COSMO_REA6/, last access: 1 June 2022.

Fox-Kemper, B., Hewitt, H. T., Xiao, C., Aðalgeirsdóttir, G., Drijfhout, S. S., Edwards, T. L., Golledge, N. R., Hemer, M., Kopp, R. E., Krinner, G., Mix, A., Notz, D., Nowicki, S., Nurhati, I. S., Ruiz, L., Sallée, J.-B., Slangen, A., and Yu, Y.: Ocean, Cryosphere and Sea Level Change., In Climate Change 2021: The Physical Science Basis. Contribution of Working Group I to the Sixth Assessment Report of the Intergovernmental Panel on Climate Change, 6, S.1211-1362, doi:10.1017/9781009157896.011., 2021.

Friedrichs, C. T.: Barotropic tides in channelized estuaries, in: Contemporary Issues in Estuarine Physics, Valle-Levinson, A. (Ed.), Cambridge University Press, 27–61, 2010.

Friedrichs, C. T.: Tidal Flat Morphodynamics: A Synthesis, Treatise on Estuarine and Coastal Science, 137–170, doi:10.1016/B978-0-12-374711-2.00307-7, 2011.

Friedrichs, C. T. and Aubrey, D. G.: Tidal propagation in strongly convergent channels, J. Geophys. Res., 99, 3321, doi:10.1029/93JC03219, 1994.

https://doi.org/10.5194/egusphere-2023-1288
Preprint. Discussion started: 22 June 2023

Friedrichs, C. T., Aubrey, D. G., and Speer, P. E.: Impacts of Relative Sea-level Rise on Evolution of Shallow Estuaries, in: Residual Currents and Long-term Transport, Cheng, R. T. (Ed.), Springer New York, New York, NY, 105–122, 1990.

Garner, G. G., Hermans, T., Kopp, R. E., Slangen, A. B. A., Edwards, T. L., Levermann, A., Nowikci, S., Palmer, M. D., Smith, C., Fox-Kemper, B., Hewitt, H. T., Xiao, C., Aðalgeirsdóttir, G., Drijfhout, S. S., Golledge, N. R., Hemer, M., Krinner, G., Mix, A., Notz, D., Nowicki, S., Nurhati, I. S., Ruiz, L., Sallée, J.-B., Yu, Y., Hua, L., Palmer, T., and Pearson, B.: IPCC AR6 Sea-Level Rise Projections. Version 20210809.: https://podaac.jpl.nasa.gov/announcements/2021-08-09-Sea-level-projections-from-the-IPCC-6th-Assessment-Report, last access: 16 May 2022.

Garrett, C., Keeley, J. R., and Greenberg, D. A.: Tidal mixing versus thermal stratification in the Bay of Fundy and gulf of Maine, Atmosphere-Ocean, 16, 403–423, doi:10.1080/07055900.1978.9649046, 1978.

Gisen, J.: Prediction in Ungauged Estuaries, 2015.

Holleman, R. C. and Stacey, M. T.: Coupling of Sea Level Rise, Tidal Amplification, and Inundation, Journal of Physical Oceanography, 44, 1439–1455, doi:10.1175/JPO-D-13-0214.1, 2014.

HTG: Empfehlungen des Arbeitsausschusses "Ufereinfassungen" Häfen und Wasserstraßen EAU 2020: (inkl. E-Book als PDF), 12. Auflage, Ernst Wilhelm & Sohn, Berlin, 700 pp., 2020.

Jay, D. A.: Green's law revisited: Tidal long-wave propagation in channels with strong topography, J. Geophys. Res., 96, 20585, doi:10.1029/91JC01633, 1991.

Jordan, C., Visscher, J., and Schlurmann, T.: Projected Responses of Tidal Dynamics in the North Sea to Sea-Level Rise and Morphological Changes in the Wadden Sea, Front. Mar. Sci., 8, 40171, doi:10.3389/fmars.2021.685758, 2021.

Kernkamp, H. W. J., van Dam, A., Stelling, G. S., and Goede, E. D. de: Efficient scheme for the shallow water equations on unstructured grids with application to the Continental Shelf, Ocean Dynamics, 61, 1175–1188, doi:10.1007/s10236-011-0423-6, 2011.

Khojasteh, D., Glamore, W., Heimhuber, V., and Felder, S.: Sea level rise impacts on estuarine dynamics: A review, The Science of the total environment, 780, 146470, doi:10.1016/j.scitotenv.2021.146470, 2021.

Rasquin, C., Seiffert, R., Wachler, B., and Winkel, N.: The significance of coastal bathymetry representation for modelling the tidal response to mean sea level rise in the German Bight, Ocean Sci., 16, 31–44, doi:10.5194/os-16-31-2020, 2020.

Ray, R. D.: A Global Ocean Tide Model from TOPEX/POSEIDON Altimetry: GOT99.2, NASA, 1999.

S. D. Smith and E. G. Banke: Variantion of the surface drag coefficient with wind speed, Q.J.R. Meteorol. Soc., 101, 656–673, 1975.

Savenije, H. H. G.: Salinity and Tides in Alluvial Estuaries: Second Completely Revised Edition, 2.6th ed., 2012.

Savenije, H. H. G., Toffolon, M., Haas, J., and Veling, E. J. M.: Analytical description of tidal dynamics in convergent estuaries, J. Geophys. Res., 113, doi:10.1029/2007JC004408, 2008.

Sehili, A., Lang, G., and Lippert, C.: High-resolution subgrid models: Background, grid generation, and implementation, Ocean Dynamics, 64, 519–535, doi:10.1007/s10236-014-0693-x, 2014.

https://doi.org/10.5194/egusphere-2023-1288
Preprint. Discussion started: 22 June 2023

Seiffert, R. and Hesser, F.: Investigating Climate Change Impacts and Adaptation Strategies in German Estuaries, Die Küste, 81, 551–563, 2014.

Sievers, J., Malte, R., and Milbradt, P.: EasyGSH-DB: Bathymetrie (1996-2016), 2020.

Simpson, J. H. and Hunter, J. R.: Fronts in the Irish Sea, Nature, 250, 404–406, doi:10.1038/250404a0, 1974.

Song, D., Wang, X. H., Zhu, X., and Bao, X.: Modeling studies of the far-field effects of tidal flat reclamation on tidal dynamics in the East China Seas, Estuarine, Coastal and Shelf Science, 133, 147–160, doi:10.1016/j.ecss.2013.08.023, 2013.

Talke, S. A. and Jay, D. A.: Changing Tides: The Role of Natural and Anthropogenic Factors, Annual review of marine science, 12, 121–151, doi:10.1146/annurev-marine-010419-010727, 2020.

van der Wegen, M.: Numerical modeling of the impact of sea level rise on tidal basin morphodynamics, J. Geophys. Res. Earth Surf., 118, 447–460, doi:10.1002/jgrf.20034, 2013.

van Rijn, L. C.: Analytical and numerical analysis of tides and salinities in estuaries; part I: tidal wave propagation in convergent estuaries, Ocean Dynamics, 61, 1719–1741, doi:10.1007/s10236-011-0453-0, 2011.

Wachler, B., Seiffert, R., Rasquin, C., and Kösters, F.: Tidal response to sea level rise and bathymetric changes in the German Wadden Sea, Ocean Dynamics, 70, 1033–1052, doi:10.1007/s10236-020-01383-3, 2020.

Winterwerp, J. C. and Wang, Z. B.: Man-induced regime shifts in small estuaries—I: theory, Ocean Dynamics, 63, 1279–1292, doi:10.1007/s10236-013-0662-9, 2013.

WSV: Zentrales Datenmanagement (ZDM): Küstendaten: https://www.kuestendaten.de/DE/Services/Messreihen_Dateien_Download/Download_Zeitreihen_node.html.

Zhou, Z., Coco, G., Townend, I., Gong, Z., Wang, Z., and Zhang, C.: On the stability relationships between tidal asymmetry and morphologies of tidal basins and estuaries, Earth Surf. Process. Landforms, 43, 1943–1959, doi:10.1002/esp.4366, 2018.

Zijl, F.: An application of Delft3D Flexible Mesh for operational water-level forecasting on the Northwest European Shelf and North Sea (DCSMv6), Deltares, NGHS Symposium, Delft Software Days, 2014, 2014.

Zijl, F., Sumihar, J., and Verlaan, M.: Application of data assimilation for improved operational water level forecasting on the northwest European shelf and North Sea, Ocean Dynamics, 65, 1699–1716, doi:10.1007/s10236-015-0898-7, 2015.

Zijl, F., Verlaan, M., and Gerritsen, H.: Improved water-level forecasting for the Northwest European Shelf and North Sea through direct modelling of tide, surge and non-linear interaction, Ocean Dynamics, 63, 823–847, doi:10.1007/s10236-013-0624-2, 2013.